Intersubband transitions in $In_xAl_{(1-x)}N/In_yGa_{(1-y)}N$ quantum well operating at 1.55 μm

Hassen Dakhlaoui†

Department of Physics, College of Science for Girls, Dammam 31113, Saudi Arabia

(Received 27 January 2014; revised manuscript received 31 March 2014; published online 23 July 2014)

In this paper, we theoretically study the effects of doping concentration N_D and an external electric field on the intersubband transitions in $In_xAl_{(1-x)}N/In_yGa_{(1-y)}N$ single quantum well by solving the Schrödinger and Poisson equations self-consistently. Obtained results including transition energies, the band structure, and the optical absorption have been discussed. The lowest three intersubband transitions (E_2-E_1), (E_3-E_1), and (E_3-E_2) are calculated as functions of doping concentration N_D. By increasing the doping concentration N_D, the depletion effect can be reduced, and the ionized electrons will compensate the internal electric field which results from the spontaneous polarization. Our results show that an optimum concentration N_D exists for which the transition 0.8 eV (1.55 μm) is carried out. Finally, the dependence of the optical absorption $\alpha_{13}(\omega)$ on the external electric field and doping concentration is studied. The maximum of the optical absorption can be red-shifted or blue-shifted through varying the doping concentration and the external electric field. The obtained results can be used for designing optical fiber telecommunications operating at 1.55 μm.

Keywords: intersubband transition, delta doping, InGaN/GaN quantum well

PACS: 73.21.Fg, 73.50.Dn, 73.50.Dn **DOI:** 10.1088/1674-1056/23/9/097304

1. Introduction

In recent years, various theoretical and experimental studies have been developed on the intersubband transitions (ISBT) in III-nitride semiconductor quantum wells because of their strong applications for optoelectronic devices, such as optical switches, quantum well photodetectors, and quantum-cascade lasers for telecommunications applications.[1–13] AlGaN/GaN has drawn considerable attention as a potential material system for the fabrication of devices based on ISBTs at telecommunications wavelength because of their large conduction band offset, which can exceed 2.0 eV and the large difference of refractive index between GaN and AlN.[14,15] In addition, the nitride semiconductor has very fast carrier dynamics. The relaxation times of the carrier are typically of the order of 150 fs because of the enhanced electron-phonon interaction. The fast relaxation time could also provide the basis for optical modulators that are very resistant to the absorption saturation. Nevertheless, growing device structures based on the GaN/AlGaN system for ISBT is challenging and has been prevented by different obstacles such as dislocations and cracks because of the lack of a lattice-matched substrate and the large lattice mismatch between AlGaN and GaN.[16–20] To solve this problem, the simple solution would be to find new materials with good lattice matching to avoid the formation of dislocations and parasitic conduction channels. With the discovery of the $In_xAl_{(1-x)}N$ alloy, the problems of dislocations have been solved. $In_xAl_{(1-x)}N$ with low indium concentration (17–20%) is lattice-matched to GaN, and the conduction band discontinuity is much broader, which is consistent with the design of heterostructures with intersubband transitions ISBT in the infrared range.[21–24] Unlike other materials, the piezoelectric polarization in $In_xAl_{(1-x)}N$-GaN interfaces is not important because of the absence of strain in the lattice-matched. The absence of the piezoelectric effect and the large conduction band offset in $In_xAl_{(1-x)}N$-GaN materials make them more accessible than other materials such as AlGaN/GaN. Among many theoretical studies, Zhou *et al.*,[23] studied the effect of single quantum well thickness on electronic properties, such as the optical absorption. They showed that it is possible to obtain the mid-infrared domain by changing the width of the quantum well and then reducing the effect of the asymmetry produced by the polarization field. In this paper, intersubband transitions and optical absorption in $In_xAl_{(1-x)}N/In_yGa_{(1-y)}N$ single quantum well are theoretically studied. Our paper is organized as follows: in Section 2, we describe the theoretical method used in this calculation. The results of the simulation and the discussion are presented in Section 3. Finally, the conclusion is given in Section 4.

2. Computational method

By using the effective mass approximation, the time-independent Schrödinger equation, which describes the motion of the electron, can be written in the following form:[25–27]

$$-\frac{\hbar^2}{2m^*}\frac{\mathrm{d}^2\Psi_i(z)}{\mathrm{d}z^2}+(V_C(z)+V_H(z)+V_{XC}(z))\Psi_i(z)=E_i\Psi_i(z), \quad (1)$$

where z represents the growth direction, m^* is the effective mass of the electron, $V_C(z)$ denotes the conduction band offset

†Corresponding author. E-mail: h_dakhlaoui@yahoo.fr

© 2014 Chinese Physical Society and IOP Publishing Ltd

between $In_xAl_{(1-x)}N$ and $In_yGa_{(1-y)}N$ and is given by[28,29]

$$V_C(z) = 0.52(2.53x^2 - 6.92x + 3.93y + 2.86)\ \text{eV}. \quad (2)$$

The exchange-correlation potential $V_{XC}(z)$ can be ignored in heterostructures with high-doped concentration.[16] $V_H(z)$ is the effective Hartree potential, which represents the electrostatic interaction of electrons with themselves and with ionized impurities. The $V_H(z)$ can be found by solving the following Poisson equation:

$$\frac{d^2V_H(z)}{dz^2} = \frac{e^2}{\varepsilon_0\varepsilon_r}\left[\frac{\sigma}{e}\delta(z-z_0) + N_D(z) - n(z)\right], \quad (3)$$

where $n(z)$ represents the electronic density of the confined electrons, $N_D(z)$ is the total doping concentration, and $\varepsilon_0\varepsilon_r$ is the dielectric constant. The electronic density is given as follows:

$$n(z) = \sum_i \frac{m^*K_BT}{\pi\hbar^2}\log\left[1+\exp\left(\frac{E_F-E_i}{K_BT}\right)\right]\Psi_i^2(z), \quad (4)$$

where K_B is Boltzmann constant, E_F denotes Fermi level, i represents the subband level index, and T is the absolute temperature. In Eq. (2), the polarization-induced charge density is taken as[28,30,31]

$$\begin{aligned}&\sigma(In_xAl_{(1-x)}N/In_yGa_{(1-y)}N)\\ &= 0.052 - 0.049x\\ &\quad + (0.132 - 0.744x - 0.032x^2)/(3.112 + 0.436x)\\ &\quad + y(0.158y + 0.488)/(3.189 + 0.359y)\,\text{C}\cdot\text{m}^{-2}. \quad (5)\end{aligned}$$

The numerical calculation also gives the Fermi level E_F, from the condition that the total number of electrons must equal the total number of donors, that is, E_F satisfies the neutrality equation

$$\sum_i n_i - N_D - \frac{1}{e}\sum_i \sigma_i = 0.$$

In our study, all donors are assumed to be ionized and are replaced by uniform distribution. We have solved Eqs. (1)–(3) self-consistently using the finite difference method.[32–34] After the confining potential, the subband energies and their corresponding wavefunctions are obtained; the optical absorption coefficient can be clearly calculated as follows:[35]

$$\begin{aligned}\alpha(\omega) &= \frac{\omega\mu ce^2}{n_r}|M_{fi}|^2\frac{m^*K_BT}{L_{eff}\pi\hbar^2}\\ &\quad\times\ln\left\{\frac{1+\exp[(E_F-E_i)/K_BT]}{1+\exp[(E_F-E_f)/K_BT]}\right\}\\ &\quad\times\frac{\hbar/\tau_{in}}{(E_F-E_i-\hbar\omega)^2+(\hbar/\tau_{in})^2}, \quad (6)\end{aligned}$$

with the matrix element

$$M_{fi} = \int_{-L/2}^{L/2}\psi_f^*(z)\,z\,\psi_i(z)\,dz,$$

where $E_{fi} = E_f - E_i$, E_f and E_i represent the energy levels for the final and initial states, respectively, μ is the permeability, C is the speed of light in free space, L_{eff} is the effective spatial extent of electrons in subbands, n_r is the refractive index, and τ_{in} is the intrasubband relaxation time (where τ_{in} is a constant and used the numerical value of 0.14 ps following Ref. [36]).

3. Results and discussion

The structure studied here consists of $Al_{0.8}In_{0.2}N$ (L_b)/GaN (L_w)/$Al_{0.8}In_{0.2}N$ (L_b) single quantum well. The quantum well and barrier widths are $L_w = 18$ Å and $L_b = 20$ Å. $m^* = 0.22m_0$, $T = 298$ K. The doping concentration is uniformly located on the left barrier, and the doping concentration is taken as a parameter N_D. The boundary conditions are $\Psi_1(0) = \Psi_1(L_w + 2L_b) = 0$. Figure 1 gives the three lowest wavefunctions, energy levels, and the conduction band profile of the single quantum well $Al_{0.8}In_{0.2}N(L_b)$/GaN(L_w)/$Al_{0.8}In_{0.2}N(L_b)$ single without doping concentration $N_D = 0$. As shown in Fig. 1, the conduction band profile is titled, and thus, the wavefunctions are slightly moved to the left side of the quantum well. This can be explained as follows: because of the spontaneous polarization charges at the interfaces $In_xAl_{(1-x)}N$/GaN, an electric field is produced along the quantum well and barriers, so the parity of the selection rule is broken, which makes the conduction band profile asymmetric. Hence, the three wave functions are pushed to the left interface of the quantum well. Figure 2 displays the three lowest intersubband transitions $(E_2 - E_1)$, $(E_3 - E_1)$, and $(E_3 - E_2)$ as functions of the doping concentration N_D. Our objective is to obtain the intersubband transition wavelength 1.55 μm (0.8 eV), which is needed in the telecommunication domain. As shown in this figure, we vary the doping concentration N_D from 4×10^{16} m^{-2} to 2×10^{17} m^{-2}. The two intersubband transitions $(E_2 - E_1)$ and $(E_3 - E_1)$ decrease with N_D; however, $(E_3 - E_2)$ increases with it. The suitable doping concentration N_D, which achieves the intersubband transition 1.55 μm (0.8 eV) is equal to 5×10^{16} m^{-2}, and it is obtained only for $(E_3 - E_1)$ transition (black line in Fig. 2).

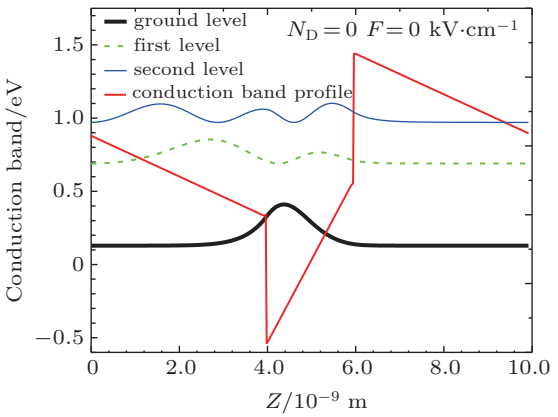


Fig. 1. (color online) Conduction band structures of doped InGaN quantum well.

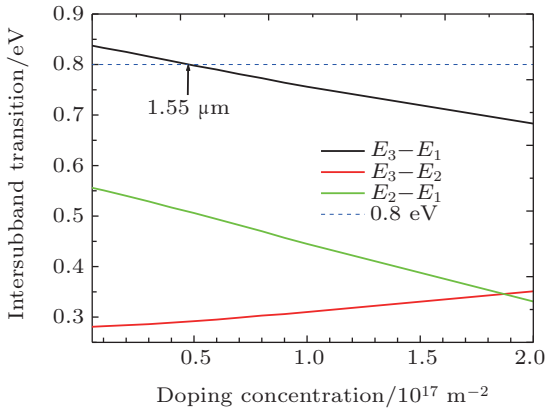


Fig. 2. (color online) Transition energy in doped quantum well.

According to Eq. (6), the square value of the matrix element $|M_{\rm fi}|^2$, the energy difference $(E_{\rm f}-E_{\rm i})$, and the Fermi occupancy ratio

$$f_{\rm i}-f_{\rm f}=\ln\left\{\frac{1+\exp[(E_{\rm F}-E_{\rm i})/K_{\rm B}T]}{1+\exp[(E_{\rm F}-E_{\rm f})/K_{\rm B}T]}\right\}$$

between the initial state (i) and the final state (f) are the three governing factors in determining the absorption coefficient value $\alpha_{\rm if}(\omega)$. We will discuss the (E_3-E_1) transition because it is the only one that gives us the wavelength of 1.55 μm. Figure 3(a) shows the square value of the matrix element $|M_{31}|^2$ as a function of doping concentration $N_{\rm D}$. $|M_{31}|^2$ increases at first and then decreases, which means that the overlap of the ground and the third excited wavefunctions is decreased when $N_{\rm D}$ increases. This means that the two wavefunctions' overlap is enlarged with $N_{\rm D}$. Figure 3(b) shows the Fermi occupancy ratio as a function of the doping concentration. By increasing $N_{\rm D}$, the Fermi occupancy ratio increases quickly, and this is due to the enhancement of the confinement, leading to the change in the difference between E_3 and E_1. In Fig. 3(c), the absorption coefficient as a function of incident frequency is given for the three values of doping concentration $N_{\rm D}$. The optical absorption peak is observed to increase in magnitude with the increase of the doping concentration. This can be interpreted as follows: from expression (6), we can see that the optical absorption is mainly determined by three factors, the energy difference (E_3-E_1), the square value of the matrix element $|M_{\rm fi}|^2$, and the Fermi occupancy ratio f_1-f_3. When $N_{\rm D}$ increases, the energy distance (E_3-E_1) decreases (Fig. 2), the Fermi occupancy ratio increases, whereas the square value of the matrix element decreases. Moreover, the contribution of the dipole matrix is not significant because its variation is so slow and can be ignored. According to these results, the optical absorption $\alpha_{31}(\omega)$ is mainly determined by the Fermi occupancy ratio and the inverse of the energy difference (E_3-E_1), which results in the magnitude of $\alpha_{31}(\omega)$ increasing with $N_{\rm D}$ and also shifting toward the lower energies. These results indicate that the doping concentration plays an important role in the design of $In_xAl_{(1-x)}N$/GaN quantum well because it can modify the Fermi occupancy ratio, which has a great influence on the optical absorption leading to the red shift.

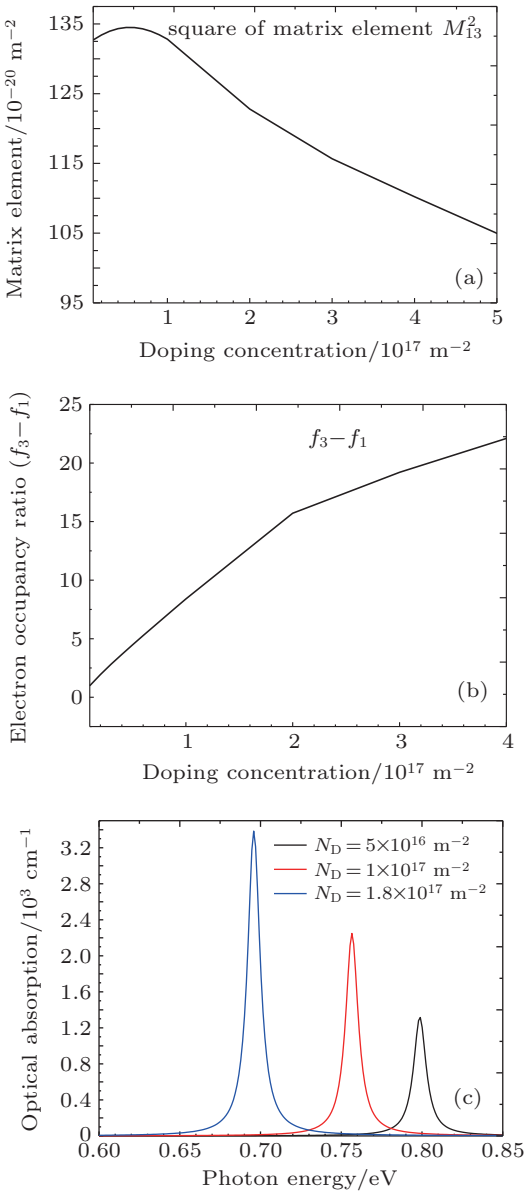


Fig. 3. (color online) (a) Square matrix element, (b) electron occupancy ratio, and (c) optical absorption $\alpha_{31}(\omega)$ as functions of doping concentration $N_{\rm D}$.

Figure 4(a) displays the optical absorption $\alpha_{31}(\omega)$ as a function of the incident photon energy for different values of the applied electric field. From this figure, the optical absorption is red shifted as the electric field is increased. In addition, the absorption peak is decreased in magnitude with electric field intensity increasing. This result can be explained as follows: when the electric field intensity increases, the third excited state decreases quickly, while the first state and the Fermi level change slowly. Thus, the occupancy ratio decreases as shown in Fig. 4(b). The optimum value of electric field to obtain the desired transition 1.55 μm is equal to 500 kV/cm.

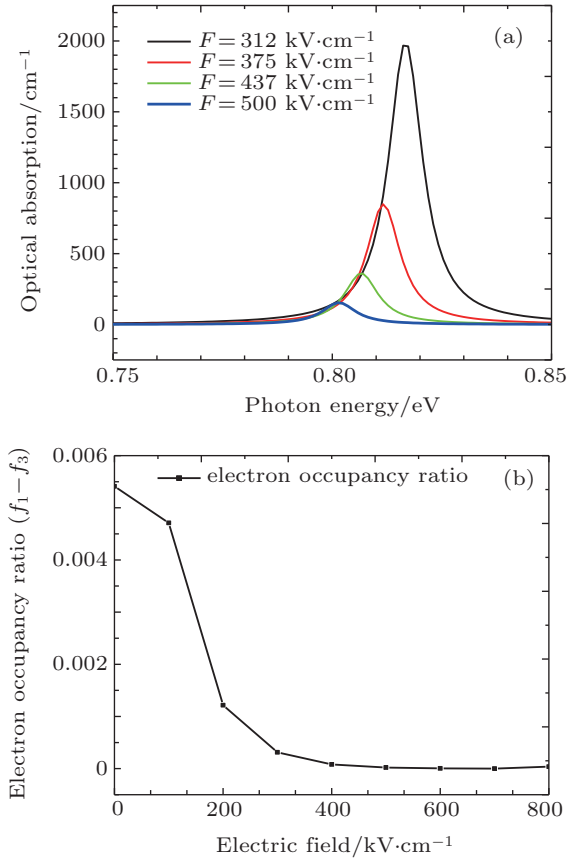


Fig. 4. (color online) (a) Optical absorption $\alpha_{13}(\omega)$ at different applied electric fields and (b) electron occupancy ratios at different applied electric fields.

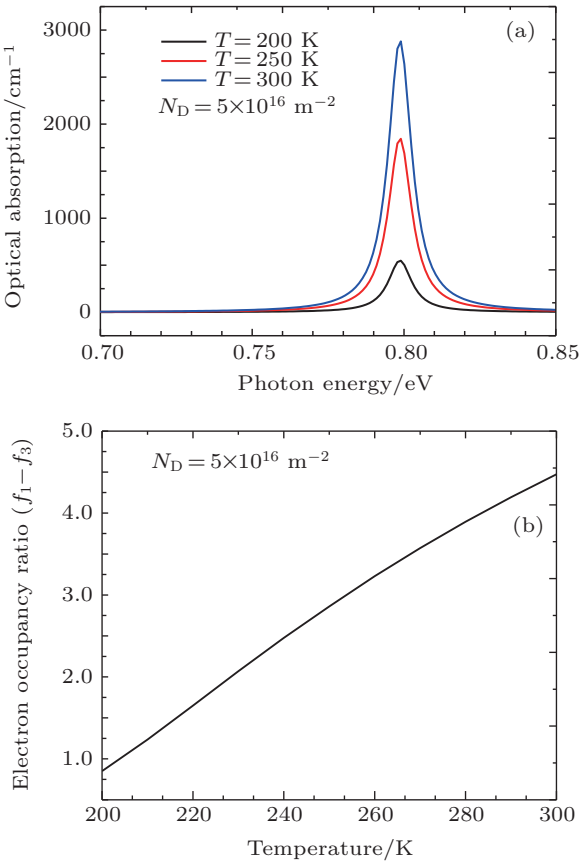


Fig. 5. (color online) (a) Optical absorption $\alpha_{13}(\omega)$ at different temperatures and (b) electron occupancy ratios at different temperatures.

Note that the applied electric field breaks the parity of the selection rule leading a conduction band profile to be asymmetric. From all the previous results, we can conclude that the occupancy ratio is an important factor, which determines the magnitude of the optical absorption. Figure 5(a) shows the variation of the optical absorption coefficient $\alpha_{31}(\omega)$ as a function of the incident photon energy at different temperatures. From this figure, the absorption peak is clearly increased in magnitude with increasing the temperature. This can be explained by the fact that the levels E_3 and E_1 are more populated when the temperature increases, but the population on E_3 is slower than that of E_1, leading to a decrease in (E_3-E_1); thus, the occupancy ratio increases, and thus, the magnitude of the absorption coefficient becomes higher.

4. Conclusions

The intersubband transitions in $Al_{0.8}In_{0.2}N$ / $GaN/Al_{0.8}In_{0.2}N$ single quantum will be very important in the applications. Using a self-consistent Schrödinger–Poisson calculation, the confining potential, the optical absorption, and the intersubband transitions were studied as functions of an external electric field and the doping concentration N_D located in the left barrier. Our numerical results show that the doping concentration and the applied electric field can play an important role in adjusting the optical absorption in the desired wavelength. We have found that the required transition 0.8 eV (1.55 μm) is carried out with a doping concentration of $5.\times10^{16}$ m^{-2}. In addition, we have found that for a fixed doping concentration, the optical absorption is red shifted as the electric field is increased. The optimum value of the electric field to obtain the desired transition wavelength (1.55 μm) is $F=500$ kV/cm. At the same time, our simulations show that by increasing the temperature, we obtain higher peak values of the optical absorption because of the great difference in the population between the first and the third excited states. Finally, our numerical results indicate that the occupancy ratio is an important factor in determining the magnitude and the peak position of the optical absorption. We hope that the present numerical results are helpful to design and construct the new devices such as optical fiber telecommunications operating at 1.55 μm.

References

[1] Iizuka N, Kaneko K and Suzuki N 2002 *Appl. Phys. Lett.* **81** 1803
[2] Hamazaki J, Kunugita H, Emna K, Kikuchi A and Kishino K 2005 *Phys. Rev. B* **71** 165335
[3] Tchernycheva M, Nevou L, Doyennette L, Julien F H, Warde E, Guillot F, Monroy E, Bellet-Amalric E, Remmele T and Albrecht M 2006 *Phys. Rev. B* **73** 125347
[4] Driscoll K, Bhattacharyya A, Moustakas T D, Paiella R, Zhou L and Smith D J 2007 *Appl. Phys. Lett.* **91** 141104
[5] Machhadani H, Kotsar Y, Sakr S, Tchernycheva M, Colombelli R, Mangeney J, Amalric E B, Sarigiannidou E, Monroy E and Julien F H 2010 *Appl. Phys. Lett.* **97** 191101

[6] Bellotti E, Driscoll K, Moustakas T D and Paiella R 2009 *J. Appl. Phys.* **105** 113103

[7] Remnev M A, Kateev I Y and Elesin V F 2010 *Semiconductors* **44** 1034

[8] Zhang W, Zhang Y, Xue J S, Zhang Y, Ling L, Zhang J C and Hao Y 2011 *Appl. Phys. Lett.* **99** 162105

[9] Ha S H, Ban S L and Zhu J 2011 *Physica B* **406** 3640

[10] Sakr S, Warde E, Tchernycheva M and Julien F H 2011 *J. Appl. Phys.* **109** 023717

[11] Lin G J, Lai H K, Li C, Chen S Y and Yu J Z 2008 *Chin. Phys. B* **17** 3479

[12] Zhang C X, Liang J Q and Nie Y H 2008 *Chin. Phys. B* **17** 2670

[13] Zhang Y H and Wang C 2006 *Chin. Phys. B* **15** 649

[14] Suzuki N and Iizuka N 1997 *Jpn. J. Appl. Appl. Phys.* **36** L1006

[15] Helman A, Tchernycheva M, Lusson A, Warde E, Julien F H, Moumanis Kh, Fishman G, Monroy E, Daudin B, Le Si Dang D , Bellet-Amalric E and Jalabert D 2003 *Appl. Phys. Lett.* **83** 5196

[16] Kikuchi A, Bannai R, Kishino K, Lee C M and Chyi J I 2002 *Appl. Phys. Lett.* **81** 1729

[17] Foxon C T, Novikov S V, Belyaev A E, Zhao L X, Makarovsky O, Walker D J, Eaves L, Dykeman R I, Danylyuk S V, Vitusevich S A, Kappers M J, Barnard J S and Humphreys C J 2003 *Phys. Status Solidi C* **0** 2389

[18] Golka S, Pflügl C, Schrenk W, Strasser G, Skierbiszewski C, Siekacz M, Grzegory I and Porowski S 2006 *Appl. Phys. Lett.* **88** 172106

[19] Bayram C, Vashaei Z and Razeghi M 2010 *Appl. Phys. Lett.* **96** 042103

[20] Nicolay S, Carlin J F, Feltin E, Butté R, Mosca M, Grandjean N, Ilegems M, Tchernycheva M, Nevou L and Julien F H 2005 *Appl. Phys. Lett.* **87** 111106

[21] Asif K M, Yang J W, Simin G, Gaska R, Shur M S, zur Loye H, Tamulaitis G, Zukauskas A, Smith D J, Chandrasekhar D and Bicknell-Tassius R 2000 *Appl. Phys. Lett.* **76** 1161

[22] Kim K S, Saxler A, Kung P, Razeghi M and Lim K Y 1997 *Appl. Phys. Lett.* **71** 800

[23] Wang Y Z, Li D, Li L, Liu N Y, Liu L, Cao W Y, Chen W H and Hu X D 2011 *Chin. Phys. B* **20** 094297

[24] Cen L B, Shen B, Qin Z X and Zhang G Y 2009 *Chin. Phys. B* **18** 3905

[25] Saidi I, Bouzaïene L, Gazzah M H, Mejri H and Maaref H 2006 *Solid State Commun.* **140** 308

[26] Li J M, Lu Y W, Li D B, Han X X, Zhu Q S, Liu X L and Wang Z G 2004 *J. Vac. Sci. Technol. B* **22** 2568

[27] Ben J A, Mejri H, Maaref H and Souissi K 1997 *Semicond. Sci. Technol.* **12** 1388

[28] Kuzmik J 2002 *Semicond. Sci. Technol.* **17** 540

[29] Jain S C, Willander M, Narayan J and Overstraeten R V 2000 *J. Appl. Phys.* **87** 965

[30] Ambacher O, Foutz B, Smart J, Shealy J R, Weimann N G, Chu K, Murphy M, Sierakowski A J, Schaff W J, Eastman L F, Dimitrov R, Mitchell A and Stutzmann M 2000 *J. Appl. Phys.* **87** 334

[31] Morkoç H, Cingolani R and Gil B 1999 *Solid State Electron.* **43** 1909

[32] Cuesta J A, Sanchez A and Dominguez-Adame F 1995 *Semicond. Sci. Technol.* **10** 1303

[33] Gmachl C, Hock M. Ng, George Chu S N and Alfred Y C 2000 *Appl. Phys. Lett.* **77** 3722

[34] Dakhlaoui H and Jaziri S 2005 *Physica B* **355** 401

[35] Wong K M and Allsopp D W E 2009 *J. Semicond. Sci. Technol.* **24** 045018

[36] Huang Y and Lien C 1995 *J. Appl. Phys.* **77** 3433